Chaotic motion of a periodically driven particle in an asymmetric potential well

R. Räty, J. von Boehm, and H. M. Isomäki
Department of General Sciences, Helsinki University of Technology, SF-02150 Espoo 15, Finland
(Received 2 January 1986; revised manuscript received 20 June 1986)

We study the chaotic motion of a particle in an asymmetric potential well, for which the equation of motion is $\ddot{x}+0.4\dot{x}+x-\beta x^2-4x^3=0.115\cos(\omega t)$. For $0\leqq\beta\lesssim 0.008$, a splitting into the right and left attractors occurs due to the symmetry rule. (This rule is fully generalized.) The left attractor does not appear for $\beta>0.008$. The ω regions of the periods of the dominating right attractor increase when β increases from 0 to $0.006,\ldots,0.008$ the increase of the ω region of period 3 ($\rightarrow 6\rightarrow 12\rightarrow\cdots$) being anomalously strong. The behavior for $0\leqq\beta\lesssim 0.006$ can be described with a cubic map. For $0.008<\beta\leq 0.1$, a steepening parabola-type return map can be found for the right attractor consistently with the fact that the calculated motion is similar to the behavior of the one-dimensional unimodal $z=2$ maps. The absence of period 3 ($\rightarrow 6\rightarrow 12\rightarrow\cdots$) appears as an abrupt steepening of the return map.

I. INTRODUCTION

The chaotic motion of a periodically driven classical particle in an anharmonic potential well (with damping) has been studied in several recent papers.[1–14] Based on the behavior of this model it has been suggested that solid-state turbulence occurs in anisotropic solids for charge-density waves oscillating with respect to the pinning impurity centers,[1] for oscillating ions in superionic conductors[1] and for oscillating straight dislocation segments.[15] The chaotic motion of a particle in a symmetric potential well—relevant for the above systems—has been studied in Refs. 1, 5, and 12. The purpose of the present paper is to extend these studies by examining the influence of an added constant driving force (or equivalently the influence of the asymmetry in the potential well) on the chaotic motion. Namely, this influence is of some importance because periodic plus constant driving forces are often used in actual experiments and/or the potential well may be directly asymmetric due to the asymmetric environment.[16] And, on the other hand, the addition of small extra driving terms may be expected to cause significant qualitative changes in chaotic motion.[17]

II. METHODOLOGY

The system to be studied has the dimensionless equation of motion

$$\ddot{x}+0.4\dot{x}+x-\beta x^2-4x^3=0.115\cos(\omega t) \tag{1}$$

that can also be transformed[18] into the form

$$\ddot{x}+0.4\dot{x}+x-4x^3=\frac{\beta}{12}+0.115\cos(\omega t)\ , \tag{2}$$

with a relative error of less than 0.001 in the coefficients when $0<\beta\leq 0.1$. Equations (1) and (2) are of the generalized Duffing type. The damping constant 0.4 and the amplitude 0.115 are the same as in Refs. 1, 5, and 12 except that a slightly larger amplitude 0.1175 is used in Ref. 5. The angular frequency ω of the periodic driving force and the asymmetry constant β are system parameters. The dimensionless potential V of the spring force of Eq. (1) is shown in Fig. 1 for $\beta=0$ (the symmetric case) and 0.1. The increase of β raises (lowers) the left (right) barrier of V [or increases the constant driving force in Eq. (2)]. Only bounded motion between the barriers will be considered.

The Runge-Kutta-Verner fifth- and sixth-order method was used in solving Eq. (1). The maximum allowed error 10^{-7} within the time step $2\pi/(60\omega)$ was used.

III. RESULTS AND DISCUSSION

Figure 2 shows the calculated amplitude response diagrams $X(\omega)$ for $\beta=0$ and 0.1 [X denotes the values of the intersections of the attractor(s) with the positive x axis]. The diagrams consist of the main resonance R and the secondary resonance R' at $\omega=\frac{1}{3}$. For $\beta=0$ there are no secondary resonances at $\omega=\frac{1}{2},\frac{1}{4},\ldots$ because our solution obeys the symmetry $x(t+\pi/\omega)=-x(t)$.[13] For decreasing ω, R is discontinuous (continuous) for $\beta=0$ (0.1). R

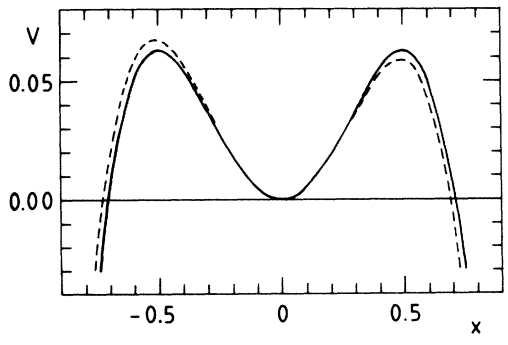

FIG. 1. Potential $\frac{1}{2}x^2-\frac{1}{3}\beta x^3-x^4$ of the nonlinear spring force for $\beta=0$ (solid line) and $\beta=0.1$ (dashed line).

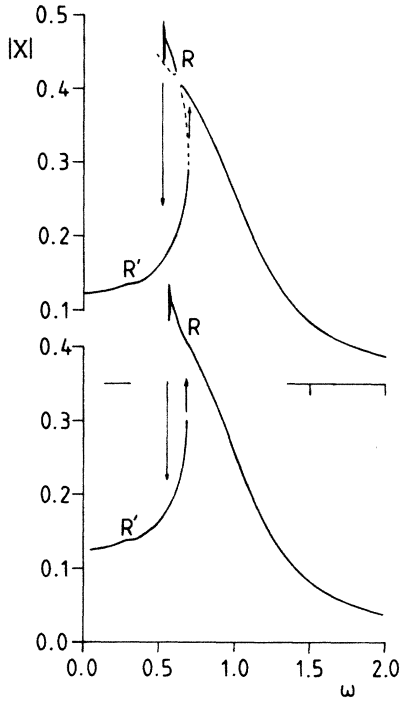

FIG. 2. Amplitude response diagram for $\beta=0$ and 0.1 (the upper and lower one, respectively). X is the value of the intersections of the attractor(s) with the positive x axis. The dashed lines represent unstable solutions.

and its discontinuity for $\beta=0$ can be understood with the Krylov-Bogoliubov theory that gives for the resonance curve the expression[19]

$$\omega^2=0.92-3X^2\pm(f^2X^{-2}-0.1536+0.48X^2)^{1/2}\,, \quad (3)$$

where 0.115 in Eq. (1) has been replaced by f. The curve has a discontinuity if

$$X^2=0.16\pm[(0.16)^2-3(1.2)^{-2}f^2]^{1/2} \quad (4)$$

has real solutions, i.e., when $f<0.064\times 3^{1/2}\approx 0.1109$. The Krylov-Bogoliubov theory predicts quite accurately the appearance of the discontinuity lying in the range $0.115<f<0.1175$ (our $f=0.115$ and $f=0.1175$ of Ref. 5 give discontinuous and continuous curves, respectively). R ends in a chaotic region (the strong line broadening in Fig. 2) that cannot be described with the Krylov-Bogoliubov method or other similar methods.

For $\beta=0$ and for decreasing ω the chaotic region is preceded by a splitting of the one inversion-symmetric attractor into two mutually inversion-symmetric attractors (right and left). The splitting is due to the symmetry rule that forbids inversion-symmetric attractors from having an even period.[12,20] (This rule is fully generalized in the Appendix.) Both attractors undergo a period-doubling cascade[21,22] to chaos where windows with both even and odd periods occur. Both chaotic attractors broaden so that they merge at $\omega\approx 0.5268$ to form again one attractor, the general form of which is inversion symmetric (an interior crisis[23,24]). After this, due to the symmetry rule, only windows with odd periods occur and their period doublings are inhibited. The jump occurs when the chaotic attractor collides with the unstable attractor (Fig. 2, a boundary crisis[23,24]).

When β is small and positive (ω decreases) a phenomenon corresponding to the symmetry-breaking splitting still exists. However, the right attractor experiencing the lower barrier develops at larger ω values than the left attractor experiencing the higher barrier (Fig. 1). Figure 3 shows as an example the two attractors for $\beta=0.001$ and $\omega=0.5281$ (the right one is already chaotic but the left one has just undergone the first period doubling). When β increases the ω region of the left attractor gradually decreases and disappears at $\beta\approx 0.008$.

The development of chaos of the dominating right attractor is shown in Fig. 4. Only the widest windows, having the periods 6, 5, and 3 ($\rightarrow 6\rightarrow 12\rightarrow\cdots$), are shown. The development of the period 2 of the right attractor is shown in Fig. 5. The ω regions of the periods in Figs. 4 and 5 grow when β grows from 0 to 0.006. . . 0.008. The ω region of the window of period 3 ($\rightarrow 6\rightarrow 12\rightarrow\cdots$) expands anomalously around $\beta\approx 0.006$ becoming approximately half the ω region of period 2 [cf. Figs. 4(b) and 5] and is about 30 times as large as at $\beta=0$. At $\beta\approx 0.008$ the window of period 3 ($\rightarrow 6\rightarrow 12\rightarrow\cdots$) disappears beyond the jump line (denoted by J in Fig. 4).

The development of chaos was studied in more detail for $\beta=0$ and 0.1. The calculated convergence numbers of the period-doubling sequences are $\Delta\omega(2)/\Delta\omega(4)=4.8$ for $\beta=0$ and $\Delta\omega(2)/\Delta\omega(4)=5.4$ and $\Delta\omega(4)/\Delta\omega(8)=5.0$ for $\beta=0.1$ indicating a limiting (geometric) convergence according to Feigenbaum's exponent $\delta\approx 4.669$ for one-dimensional (1D) unimodal ($z=2$) maps.[25,26]

The widest calculated windows with their "right-left (R-L) orders" are given in Table I.[27] Figure 6 shows, as an example, the construction of the R-L order of period 7 for $\beta=0.1$. (The same R-L orders were also obtained from the intersections with the positive x axis.)

For $\beta=0$ the sequence of periods with their R-L orders in Table I agrees with the universal (U) sequence of

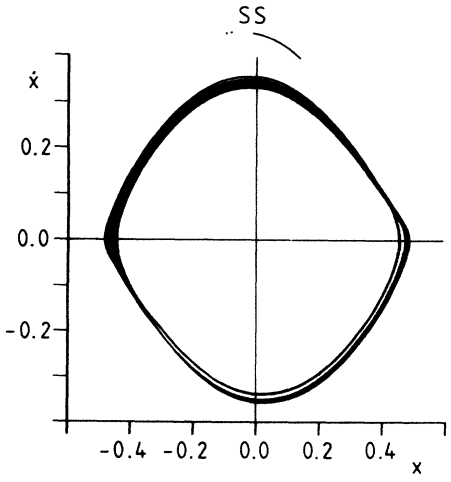

FIG. 3. Two attractors (chaotic and period 2) for $\beta=0.001$ and $\omega=0.5281$. The patterns denoted by SS are the corresponding stroboscopic sections (with $t_0=0$) shifted by 0.1 upwards.

Metropolis, Stein, and Stein[28] (MSS) for 1D unimodal ($z=2$) maps. The two last periods 7 and 5 appear after the return of the inversion symmetry (the dotted line). For $\beta=0.1$ the sequence of the periods with their R-L orders (Table I) agrees with the MSS U sequence[28] except at the dotted line where the window of period 3 ($\rightarrow 6 \rightarrow 12 \rightarrow \cdots$) is missing [cf. Fig. 4(a)].

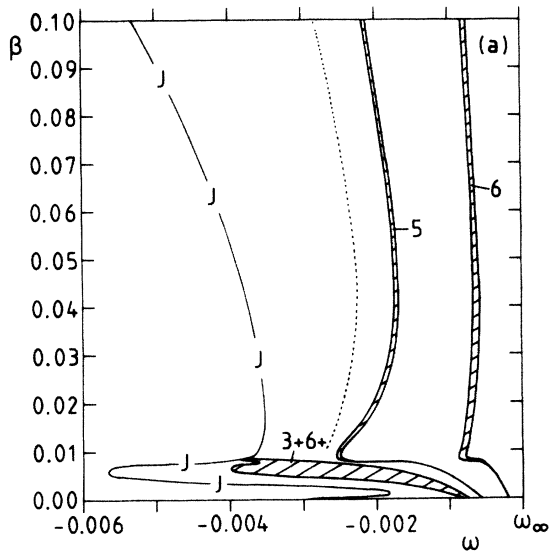

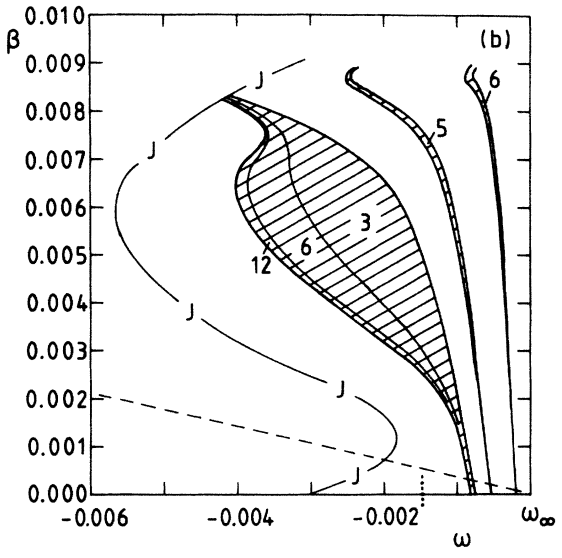

FIG. 4. Chaotic behavior of the right attractor. ω_∞ denotes the onset of chaos (placed at the right edge). $\omega_\infty(\beta=0)\approx 0.5282$ and $\omega_\infty(\beta=0.1)\approx 0.5713$. J denotes the jump (cf. Fig. 2). The dashed line in (b) represents ω_∞ of the left attractor. The dotted lines represent in (a) the place where the window of period 3 ($\rightarrow 6 \rightarrow 12 \rightarrow \cdots$) should exist and in (b) the point of the return of the inversion symmetry.

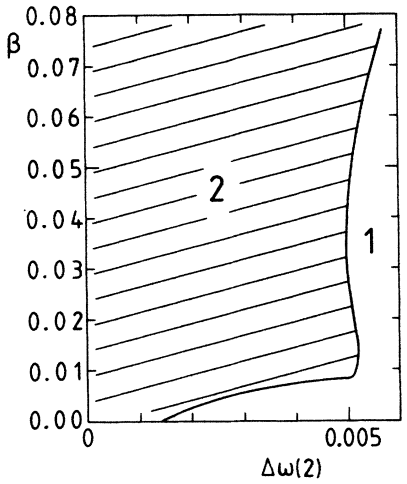

FIG. 5. Behavior of period 2 of the right attractor. $\Delta\omega(2)$ denotes the width of period 2.

IV. ONE-DIMENSIONAL ANALYSIS

One-dimensional analysis[29–32] is used for the present problem [Eqs. (1) and (2)]. The stroboscopic map—based on the Poincaré sections at $t_n = n\times 2\pi/\omega + t_0$, $n=0,1,2,\ldots$— is two-dimensional (and invertible),

$$\begin{aligned} x(t_{n+1}) &= F_{t_0}(x(t_n),\dot{x}(t_n)) \\ \dot{x}(t_{n+1}) &= G_{t_0}(x(t_n),\dot{x}(t_n)) \end{aligned} \tag{5}$$

and depends on the initial time t_0. The corresponding return map is obtained from Eq. (5) by relating the x coordinates,

$$x(t_{n+1}) = f_{t_0}(x(t_n)) \,. \tag{6}$$

Since the attractors have approximately one loop round the origin in the time $2\pi/\omega$ it is also possible to form a return map by relating the successive intersections of the

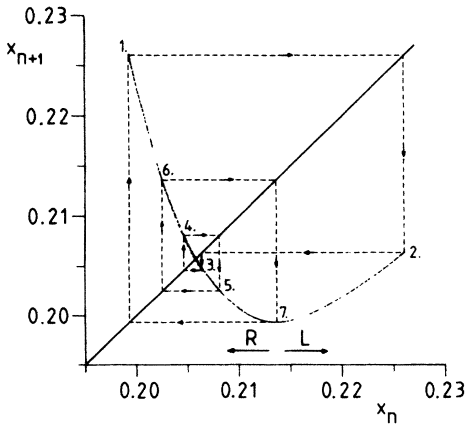

FIG. 6. Construction of the right-left (R-L) structure for the window of period 7 ($\beta=0.1$, $\omega\approx 0.5697$). The return map is based on the stroboscopic section (cf. Fig. 3).

TABLE I. Widest windows and their R-L orders. The periods up to 7 and 10 for $\beta=0$ and 0.1, respectively, are considered. The vertical arrows denote period doublings. The dotted lines denote the return of the inversion symmetry for $\beta=0$ and the place where period 3 ($\rightarrow 6$) should exist for $\beta=0.1$.

$\beta=0$		$\beta=0.1$	
2	R	2	R
4 ↓	RLR	4 ↓	RLR
6	RLR^3	8 ↓	RLR^3LR
5	RLR^2	10	RLR^3LRLR
3	RL	6	RLR^3
6 ↓	RL^2RL	7	RLR^4
5	RL^2R	5	RLR^2
4	RL^2	10 ↓	RLR^2LRLR^2
. . .	. . .	7	RLR^2LR
7		. . .	. . .
5		9	RL^2RLR^2L
		5	RL^2R
		4	RL^2

attractor(s) with the positive x axis,

$$x_{n+1}=g(x_n)\ . \tag{7}$$

The maps of Eqs. (6) and (7) have rather one-dimensional patterns (see, e.g., Fig. 6) though they have a small Cantor-set-type width and though a close second branch develops in the chaotic region. Both the map of Eq. (6) with $t_0=0$ and that of Eq. (7) are used in this paper.

For $\beta=0$ the return map [Eq. (6), $t_0=0$] resembles, after the return of the inversion symmetry, a cubic map with a minimum followed by a maximum for increasing x (cf. Ref. 5). A cubic map of this type ($-x^3+bx$) was suggested by Holmes.[2] However, a constant must be added to account for the asymmetry. The map

$$f(x)=-3x^3+bx+c\ , \tag{8}$$

studied by Kapral and Fraser,[32] will be adopted here. We review shortly the basic properties of the map [Eq. (8)] as given in Ref. 32 and complete its theory for our purposes. In Eq. (8) the increase of b ($\geqq 0$) and c ($\geqq 0$) corresponds to the decrease of ω and the increase of β in our system, respectively.

Figure 7(a) shows the map in the symmetric case ($c=0$). For increasing b, $f'(0)=b$ increases to one at $b=1$, and the fixed point of period 1 at $x=0$ splits symmetrically into two stable fixed points N and P,

$$x_{N,P}=\mp[(b-1)/3]^{1/2}\ , \tag{9}$$

both having period 1. This corresponds to the symmetry-breaking splitting in our system. Both fixed points have their own basins, the repelling origin acting as the separatrix. When b increases to $b=2$, $f'(x_N)=f'(x_P)=-1$, and both fixed points bifurcate into two periodic points, i.e., the period is doubled $1\rightarrow 2$ [see Fig. 7(a)]. When b grows to $5^{1/2}\approx 2.236$ the second period doubling $2\rightarrow 4$ occurs. Both attractors continue period doublings to chaos according to Feigenbaum's universality theory for 1D unimodal ($z=2$) maps[25,26] and the chaotic region is interrupted by periodic windows according to the MSS U sequence.[28] This behavior is the same as in our system. At $b=3\times 3^{1/2}/2\approx 2.598$ the iterates from the minimum and the maximum of the cubic map reach the origin and one might be tempted to associate this with the return of the inversion symmetry (and one attractor) in our system. However, for $b\geqq 3\times 3^{1/2}/2$ there are still two attractors the basins of which are interlaced in a complex way,[33] and the cubic map ceases to describe our system.

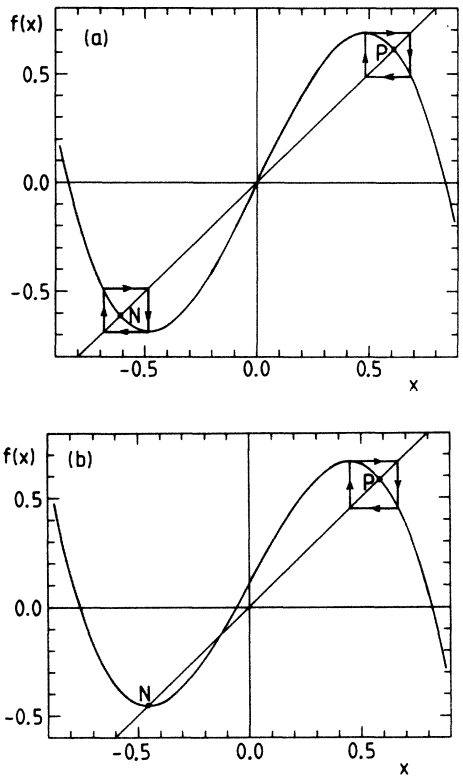

FIG. 7. Cubic map $f(x)=-3x^3+bx+c$. (a) Coexisting superstable periods 2, $b=2.12132$, $c=0$. (b) Coexisting superstable periods 1 and 2, $b=1.85063$, $c=0.105997$.

In the asymmetric case ($c>0$), P starts to develop earlier (at lower b) than N similarly to our system [see Fig. 7(b)]. The region of the window of period n in the b-c plane is determined by the equations

$$\begin{aligned} f^{(n)}(x)&=x \\ f^{(n)'}(x)&=\pm 1\ , \end{aligned} \tag{10}$$

where $f^{(n)}(x)=f^{(n-1)}(f(x))$, $+1$ corresponds to a tangent bifurcation (creation of n stable-unstable pairs of periodic points) and -1 corresponds to a period doubling ($n\rightarrow 2n$). A superstable curve of period n is obtained replacing ± 1 by 0 in Eqs. (10). Equations (10) can be solved for the periods 1 and 2 at x_P. The solutions are in the b-c

region used for comparison as follows: tangent bifurcation for 1,

$$c=\tfrac{2}{9}(b-1)^{3/2}, \tag{11}$$

superstable 1 (s1),

$$c=\tfrac{2}{9}b^{1/2}\times(b-\tfrac{3}{2}), \tag{12}$$

period doubling 1→2,

$$c=\tfrac{2}{9}(b+1)^{1/2}(2-b), \tag{13}$$

superstable 2 (s2),

$$c=-\frac{b^{1/2}}{6}(\tfrac{4}{3}b+1)+\tfrac{1}{2}(b+\tfrac{4}{3})^{1/2}, \tag{14}$$

period doubling 2→4,

$$c=\tfrac{1}{36}[12+10b+2(9b^2+12b-4)^{1/2}]^{1/2}\times[6+b-(9b^2+12b-4)^{1/2}]. \tag{15}$$

The broadening of the b region of period 2 for increasing asymmetry [b decreases in Eqs. (13)–(15)] can be understood as follows. The slopes of the superstable 2 curve and the period doubling 1→2 boundary are determined by the derivatives from Eqs. (14) and (13),

$$c'_{s2}=-\tfrac{1}{12}b^{-1/2}-\tfrac{1}{3}b^{1/2}+\tfrac{1}{4}(b+\tfrac{4}{3})^{-1/2}, \tag{16}$$

$$c'_{1\to2}=-\tfrac{1}{3}b(b+1)^{-1/2}. \tag{17}$$

For $b=2$ (at which value the period-doubling 1→2 boundary intersects the b axis), $c'_{s2}=\frac{1}{4}\times(3/10)^{1/2}-\frac{3}{8}\times2^{1/2}\approx-0.393$ and $c'_{1\to2}=-\frac{2}{9}\times3^{1/2}\approx-0.385$, i.e., the slopes are almost the same. For $b\to0$, $c'_{s2}\to-\infty$ and $c'_{1\to2}\to-0$, which has a growing effect on the distance between the superstable 2 curve and the period-doubling 1→2 boundary. It can be derived in the same way from Eq. (15) that $c'_{2\to4}\to-\infty$ when $b\to\frac{2}{3}(2^{1/2}-1)\approx0.276$ which in turn indicates growing between the period-doubling 2→4 boundary and the superstable 2 curve. A similar growing tendency for increasing asymmetry (increasing c) is also reflected in higher periods. This growing is displayed for the periods 2 and 3 in the $(b-b_{2\to4},c)$ plane in Fig. 8. The behavior of these periods is similar to that of the corresponding periods of our system for $0<\beta<0.006$ [Figs. 4(b) and 5]. However, the growing of the b region of period 3 is quantitatively about one decade weaker than that of the ω region of period 3 of our system. Since the period-doubling 1→2 boundary [Eq. (13)] has the maximum at $b=0$, $c=\frac{4}{9}$ the map ceases to describe the right attractor of our system for $c>\frac{4}{9}$ (Fig. 8).

For $\beta>0.008$—after the disappearance of the left attractor—the return map of the remaining right attractor [Eq. (6) with $t_0=0$ or Eq. (7)] has for decreasing ω a steepening unimodal form. The development of the map for $\beta=0.1$ is shown in Fig. 9 (see also Fig. 6). The steepening is consistent with our observations that the period doubling to chaos converges according to Feigenbaum's δ and that the appearance of the periodic windows follows the MSS U sequence.[25,26,28] However, the widest window of period 3 (→6→12→ ···) is missing [Fig. 4(a) and Table I]. This is not a pecularity of our system but a corresponding deviation occurs also in other oscillators. For example, in the reverse bifurcation sequence of the impact oscillator the window of period 3×2^3 is the widest of the windows in the 2^3-band but the window of period 3×2^2 is missing from the 2^2-band.[34] A similar disappearance of the window of period 3×2^2 occurs in the Henon map.[35] The developing second branch of the return map plays a significant role in the region at $\omega\approx0.5682$ where the window of period 3 (→6→12→ ···) is missing. The second branch follows closely the already existing branch for $\omega>0.5682$ (see Figs. 9 and 6). However, at $\omega\approx0.5682$ the second branch develops abruptly a minimum distinctly below the existing minimum and the return map shrinks at the same time into the three segments shown in Fig. 9 (segment 2 being the new minimum). This abrupt change is consistent with the absence of the window of period 3 (→6→12→ ···) and the three segments correspond to a chaotic three-band attractor following this window.

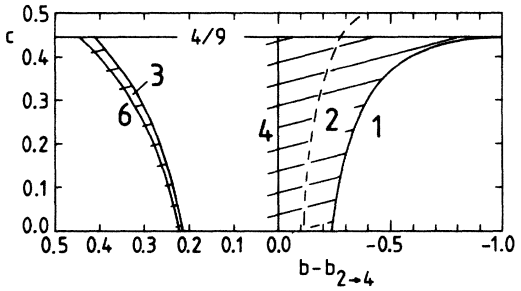

FIG. 8. Behavior of the periods 2 and 3 of the cubic map $f(x)=-3x^3+bx+c$. $b_{2\to4}$ denoting the value of the period doubling 2→4 is placed at the origin. Notice the scale change at the origin.

V. CONCLUSIONS

For $0\leqq\beta\lesssim0.008$ and decreasing ω a splitting into the right and left attractors occurs due to (or reminiscent of) the symmetry rule. (This rule is fully generalized in the

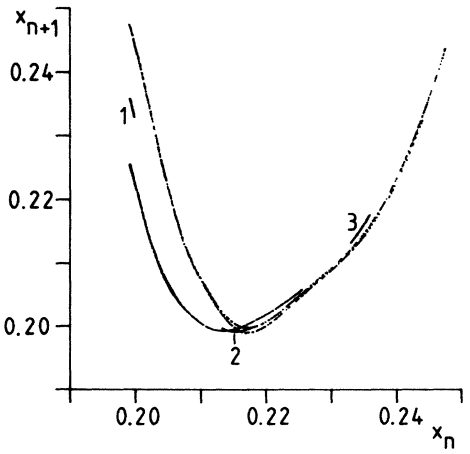

FIG. 9. Development of the return map for $\beta=0.1$. The three patterns are calculated—starting from the left—at $\omega=0.5698$, 0.5682 (parts 1, 2, and 3), and 0.566 35. The patterns are based on Eq. (6) with $t_0=0$.

Appendix). For increasing β the ω region of the left attractor decreases until this attractor disappears at $\beta \approx 0.008$. The ω regions of the periods of the dominating right attractor increase for increasing β from 0 to $0.006, \ldots, 0.008$. The above behavior for $0 \leqq \beta \lesssim 0.006$ can be described with a cubic map $-3x^3+bx+c$. However, the b region of the period 3 of this map grows much more weakly than the ω region of the period 3 ($\rightarrow 6 \rightarrow 12 \rightarrow \cdots$) of our system. The latter growth ought to be seen in experiments.

For $0.008 < \beta \lesssim 0.1$ a steepening parabola-type return map can be found for the remaining right attractor consistently with the fact that the calculated chaotic motion is similar to the behavior of the 1D unimodal ($z=2$) maps. However, the absence of period 3 ($\rightarrow 6 \rightarrow 12 \rightarrow \cdots$) appears as an abrupt steepening in the return map.

ACKNOWLEDGMENTS

The authors would like to thank M. A. Ranta and T. Aalto for their support and W. Lauterborn, R. Kapral, U. Parlitz, J. Kurkijärvi, and J. A. Ketoja for discussions. This work was supported by the Academy of Finland.

APPENDIX: GENERALIZATION OF THE SYMMETRY RULE

Consider the equations of motion

$$\dot{\underline{X}}(t)=\underline{F}(x(t),t) . \tag{A1}$$

$\underline{X}=(x_1,x_2,\ldots,x_N)^{\mathrm{tr}}$ and $\underline{F}$ are $N\times 1$ column matrices and x denotes $x_1,x_2,\ldots,x_N$. Let $\underline{F}$ have the symmetry

$$\underline{F}(x,t+\tau)=\underline{F}(x,t) , \tag{A2a}$$

$$\underline{F}(x,t+\tau/2)=-\underline{F}(-x,t) \tag{A2b}$$

(τ is the driving period). If $x(t)$ satisfies Eq. (A1), then so does $\tilde{x}(t)=-x(t+\tau/2)$. Thus the phase portraits of $x(t)$ and $\tilde{x}(t)$ are inversions of each other and coincide in the inversion-symmetric case.

Consider an inversion-symmetric periodic attractor of period T having the property

$$x(t+T/2)=-x(t) . \tag{A3}$$

[For systems based on Newton's equations of motion, Eq. (A3) follows from the inversion symmetry of the phase portrait.] The substitution $t+T/2\rightarrow t$ in Eq. (A1) and the time derivative of Eq. (A3) give

$$\dot{\underline{X}}(t)=-\underline{F}(-x(t),t+T/2) . \tag{A4}$$

Equations (A1), (A2b), and (A4) give

$$\underline{F}(x(t),t)=\underline{F}(x(t),t+T/2+\tau/2) . \tag{A5}$$

It follows from Eqs. (A2a) and (A5) that $T=(2n-1)\tau$ (with $n=1,2,3,\ldots$). This gives the generalized symmetry rule: The period of an inversion-symmetric periodic attractor must be odd. [The case that the rule does not follow from Eq. (A5) is exceptional because Eq. (A5) would then set extra time-dependent conditions between $x_i(t)$.]

[1]B. A. Huberman and J. P. Crutchfield, Phys. Rev. Lett. **43**, 1743 (1979).
[2]P. Holmes, Philos. Trans. R. Soc. London, Ser. A **292**, 419 (1979).
[3]Y. Ueda, J. Stat. Phys. **20**, 181 (1979).
[4]Y. Ueda, Ann. N.Y. Acad. Sci. **357**, 422 (1980).
[5]R. Kapral, M. Schell, and S. Fraser, J. Phys. Chem. **86**, 2205 (1982).
[6]J. Testa, J. Pérez, and C. Jeffries, Phys. Rev. Lett. **48**, 714 (1982).
[7]F. T. Arecchi and F. Lisi, Phys. Rev. Lett. **49**, 94 (1982).
[8]S. Sato, M. Sano, and Y. Sawada, Phys. Rev. A **28**, 1654 (1983).
[9]J. N. Elgin, D. Foster, and S. Sarkar, Phys. Lett. **94A**, 195 (1983).
[10]F. T. Arecchi and A. Califano, Phys. Lett. **101A**, 443 (1984).
[11]F. T. Arecchi, R. Badii, and A. Politi, Phys. Lett. **103A**, 3 (1984).
[12]R. Räty, J. von Boehm, and H. M. Isomäki, Phys. Lett. **103A**, 289 (1984).
[13]U. Parlitz and W. Lauterborn, Phys. Lett. **107A**, 351 (1985).
[14]F. T. Arecchi, R. Badii, and A. Politi, Phys. Rev. A **32**, 402 (1985).
[15]C. Herring and B. A. Huberman, Appl. Phys. Lett. **36**, 975 (1980).
[16]See, e.g., *The Physics of Superionic Conductors and Electrode Materials*, edited by J. W. Perram (Plenum, New York, 1983).
[17]K. Wiesenfeld and B. McNamara, Phys. Rev. Lett. **55**, 13 (1985).
[18]C. Hayashi, *Nonlinear Oscillations in Physical Systems* (McGraw-Hill, New York, 1964), p. 120.
[19]F. Dincă and C. Teodosiu, *Nonlinear and Random Vibrations* (Editura Academiei & Academic, Bucuresti, 1973).
[20]J. W. Swift and K. Wiesenfeld, Phys. Rev. Lett. **52**, 705 (1984).
[21]R. M. May, Nature (London) **261**, 459 (1976).
[22]S. Grossmann and S. Thomae, Z. Naturforsch. **32a**, 1353 (1977).
[23]C. Grebogi, E. Ott, and J. A. Yorke, Phys. Rev. Lett. **48**, 1507 (1982).
[24]C. Grebogi, E. Ott, and J. A. Yorke, Physica **7D**, 181 (1983).
[25]M. J. Feigenbaum, J. Stat. Phys. **19**, 25 (1978).
[26]M. J. Feigenbaum, J. Stat. Phys. **21**, 669 (1979).
[27]For $\beta=0.1$ the windows are easier to detect because the chaotic region is expanded on the ω axis compared with the $\beta=0$ case.
[28]N. Metropolis, M. L. Stein, and P. R. Stein, J. Comb. Theory (A) **15**, 25 (1973).
[29]E. N. Lorenz, J. Atmos. Sci. **20**, 130 (1963).
[30]K. Tomita and T. Kai, J. Stat. Phys. **21**, 65 (1979).
[31]K. Fesser, A. R. Bishop, and P. Kumar, Appl. Phys. Lett. **43**, 123 (1983).
[32]R. Kapral and S. Fraser, J. Phys. Chem. **88**, 4845 (1984).
[33]F. T. Arecchi, R. Badii, and A. Politi, Phys. Rev. A **29**, 1006 (1984).
[34]H. M. Isomäki, J. von Boehm, and R. Räty, in Proceedings of the International Conference on Vibration Problems in Engineering (ICVPE), edited by Du Qinghua (Tiaotong University, Xi'an, 1986), p. 326; and (unpublished).
[35]J. A. Ketoja and J. Kurkijärvi, Phys. Rev. A **33**, 2846 (1986); and (private communication).